Journal of the European Ceramic Society 21 (2001) 1485–1490

www.elsevier.com/locate/jeurceramsoc

Processing of advanced electroceramic components by fused deposition technique

M. Allahverdi, S.C. Danforth, M. Jafari, A. Safari *

Rutgers, The State University of New Jersey, Department of Ceramic and Materials Engineering, Piscataway, NJ 08854-8065, USA

Received 4 September 2000; received in revised form 14 November 2000; accepted 30 November 2000

Abstract

A variety of advanced ceramic components were fabricated using the fused deposition of ceramics (FDC) process. In FDC, ceramic loaded polymer filaments are used to build parts in a layer-by-layer fashion. A process map, based on the compressive strength and modulus of the FDC feedstock, was developed to predict the feasibility of deposition with a variety of FDC filaments. Alumina structures with photonic bandgap properties were deposited for high frequency (GHz) applications. Net shape bismuth titanate components with oriented grains were fabricated by pre-alignment of small volume of seeds in green FDC parts, followed by grain growth treatment. Piezoelectric actuators with novel structures such as spiral and bellows were manufactured and studied.

Keywords: Actuators; Piezoelectric properties; Rapid prototyping; Sensors; Shaping

1. Fused deposition of ceramics and multimaterials

Layered manufacturing or solid freeform fabrication (SFF) refers to various rapid prototyping techniques where three-dimensional (3-D) components are directly built, layer-by-layer, from a computer data description or computer aided design (CAD) files. Due to the reduced lead-time and lower cost in developing new products, the SFF techniques are valued by the commercial sectors. Over the last decade, several SFF techniques have been developed to produce polymer, metal, or ceramic components. Many of these techniques such as strereolithography (SLA),[1] selective laser sintering (SLS),[2] fused deposition modeling (FDM™),[3] and 3-D printing[4] were originally tailored to manufacture plastic parts.

In recent years, various SFF techniques such as, SLA, SLS, FDM™, and Micropen™ technology[5] have been modified and used for direct production of functional metal and ceramic parts.[6–8] Among these techniques, fused deposition (FD), has shown great promise. In the FD process (Fig. 1), feedstock in the form of spooled filaments is fed into a heated liquefier via a set of computer-driven counter-rotating rollers. The liquefier motion is computer controlled in the X–Y plane, where the material is extruded through a fine nozzle on a fixtureless platform, moving in the Z direction.

Fused deposition of ceramics (FDC), developed at Rutgers University,[9] is based on FDM™ technology where ceramic loaded polymer filaments are used for the fabrication of green ceramic components. Over the past few years, significant technical success has been achieved with functional ceramics such as silicon nitride, alumina, hydroxyapatite, lead–zirconate–titanate (PZT), and lead–magnesium niobate (PMN), as well as stainless steel and silver–palladium electrode. Normally, in the FDC process, a single material is deposited. Recently, we have developed the fused deposition of multimaterials (FDMM) process to fabricate components with up to four different materials.[10] A modified fused deposition machine (3-D Modeler™, Stratasys Inc., Eden Prairie, MN) and FDMM system were used to build a variety of functional ceramics, some of which are presented below.

2. Feedstock (filament) fabrication

(A) Binder development. To fabricate reliable FDC feedstocks, high quality thermoplastic binders suitable for fused deposition must be synthesized. We have

* Corresponding author. Tel.: +1-732-445-4367; fax: +1-732-445-5577.

E-mail address: safari@rci.rutgers.edu (A. Safari).

0955-2219/01/$ - see front matter © 2001 Published by Elsevier Science Ltd.
PII: S0955-2219(01)00047-4

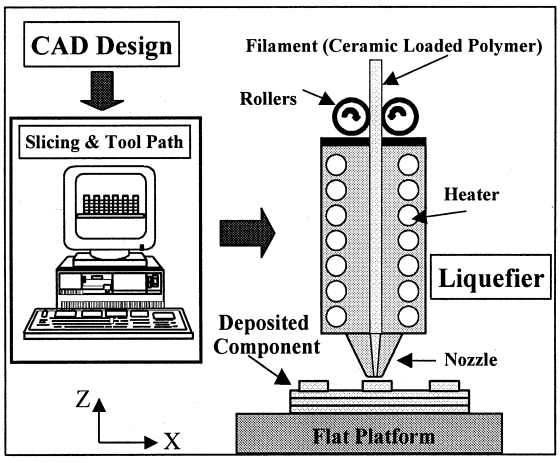

Fig. 1. Schematic of fused deposition process, including CAD file design, slicing and tool-path generation, and deposition on a platform in a layer-by-layer fashion.

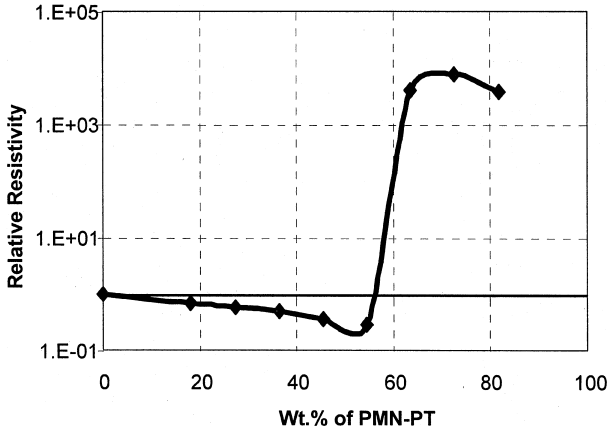

Fig. 2. Relative resistivity of the silver–palladium mixtures versus ceramic filler (PMN–PT) content. Large amount of filler (55 wt.%) can be added without increasing the resistivity of the electrode material.

developed a new family of thermoplastic binders consisting of a base binder, tackifier, wax, and plasticizer.[11] Since the new binder system (referred to as ECG series) was a multi-component system, the compatibility (e.g. thermal characteristics) of each constituent was critical. Other desirable characteristics include high strength, high stiffness, low residue after burnout, and a relatively low melt viscosity.

Evaluation of the ECG binder series[12] showed that ECG9 was the most promising one for the FDC process. ECG9 binder was utilized successfully in the fabrication of a variety of ceramic and metal filaments including soft and hard PZT[13], PMN–PT, alumina, hydroxyapatite, stainless steel, and silver palladium. All these materials were processed through the binder removal stage with no cracking or blistering. A detailed description of binder development is presented elsewhere.[12]

(B) Development of high temperature electrode filament. A high temperature silver–palladium filament was developed to lay down electrodes during fused deposition of electromechanical components. An Ag–Pd alloy powder with 49.5 wt.% palladium was used. Due to different sintering rate and shrinkage of the metal electrode relative to the ceramic, filler powders are normally added to electrode pastes or inks. We have chosen PMN–PT powder as the "filler material" for the electrode filament. In order to find the optimum level of filler addition to the electrode, a series of experiments was conducted. Fig. 2 illustrates the variation of resistivity of the electrode material versus wt.% of PMN–PT filler. It is seen that the filler can be incorporated into the electrode up to about 56 wt.% while maintaining the same level of resistivity. Based on these data, a mixture of 45 wt.% Ag–Pd and 55 wt.% PMN–PT was selected for the fabrication of high temperature electrode material.

In the first step of filament fabrication, silver–palladium powder was coated with Solsperse 13940 (Solsperse Hyperdispersants, Zeneca, NC), whereas the PMN–PT powder was coated with stearic acid. The coated powders were mixed and compounded with ECG9 binder. The solids loading of the filament was adjusted to obtain a 55 vol.% filament with approximately 23 vol.% Ag–Pd, 32 vol.% filler (PMN–PT) and 45 vol.% ECG9 binder. Electrode filament with diameter of 1.78 mm was extruded (pieces of about 1.5 feet long) using a rheometer attached to an Instron machine. The high content of palladium permits co-firing of the ceramic and electrode at a sintering temperature of about 1200°C.

3. FDC Process map

A process map, representing filament performance has been developed. The map is based on two important parameters, namely the pressure needed to drive the extrusion in FDC, and compressive elastic modulus of the filament.

The compressive modulus of FDC filaments was measured using a miniature materials tester at displacement rates of 0.1, 1, 5, 10, and 20 mm/min. The aspect ratio (L/D) of the filament samples was 1.5 in compression tests. The viscosity of the feedstock materials was characterized using a capillary rheometer at the temperatures used to deposit each material in the FDC process. Various filaments were characterized for pressure drop (ΔP) across FDC nozzles, as well as rheological properties.

Several FDC feedstocks including PZT–ECG9, Si_3N_4–RU955*, and graphite–ECG9 with different surfactants were used for the study on mechanical and rheological properties. In the stress–strain curves of

* Si_3N_4–RU955 represents a proprietary binder system (RU binders) with 55 vol,% Si_3N_4 loading.

various filaments, the slope of the initial linear region is selected as the compressive modulus of the material. The compressive modulus of a few filaments and the dependence on displacement rate showed that PZT–ECG9, graphite–ECG9, and graphite–ECG9-SA (stearic acid) exhibit a modest but statistically significant increase in compressive modulus with displacement rate. In contrast, all the other materials do not exhibit a significant dependence of compressive modulus on displacement rate.[14]

Prediction of buckling in FDC is possible by plotting $\Delta P/E$ as a function of various parameters. Fig. 3 shows the process performance indicator, $\Delta P/E$, for 52 vol.% PZT–ECG9 as a function of volumetric flow rate for different nozzle geometries (diameter and length/diameter ratio). The line corresponding to $\Delta P_{cr}/E$ is also plotted on the process map. If $\Delta P_{CT}/E$ exceeds $\Delta P_{cr}/E$ buckling should occur in the FDC process (shaded region). The process map predicts that with increasing volumetric flow rates, the tendency to buckle in FDC increases, as has been confirmed via experiments. A series of experiments also established that 52 vol.% PZT–ECG9 does not buckle, even at very high volumetric flow rates in FDC for the 0.508 mm diameter nozzle. This is predicted by the fact that the curve corresponding to the 0.508 mm diameter nozzle for 52 vol.% PZT–ECG9 lies well below the critical limit, even up to very high flow rates. The process map is a valuable tool to predict the behavior of new FDC filaments and/or deposition conditions.

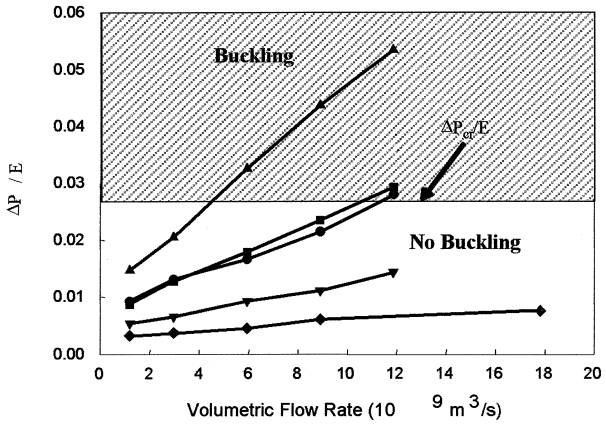

Fig. 3. Process map showing the performance indicator ($\Delta P/E$) as a function of volumetric flow rate for (◆) 0.508 mm diameter, 0.508 mm long FDC nozzle; (▼) 0.381 mm diameter, 0.381 mm long FDC nozzle; (●) 0.254 mm diameter, 0.254 mm long FDC nozzle; (■) 0.254 mm diameter, 0.508 mm long FDC nozzle; and (▲) 0.254 mm diameter, 1.27 mm long FDC nozzle, (—) $\Delta P_{cr}/E$ as a function of flow rates for all nozzle geometry.[14].

4. Net shape components with oreinted microstructures

Recently, a novel technique referred to as templated grain growth (TGG) has been implemented to create oriented grain structures in variety of ceramics.[15,16] Grain oriented microstructures are beneficial since improved mechanical and/or electrical properties can be obtained as a result of crystal anisotropy. Our objective is to combine the method of templated grain growth with the FDC process to fabricate net shape electromechanical components with superior properties. In order to achieve primary orientation in the TGG process, small percentage of anisometric (i.e. needle or platelet) seed particles must be initially incorporated and oriented within the fine powder matrix. Thus, a fabrication method with shear mechanism is required. Tape casting has been normally employed, where the slurry including 5–15 vol.% seeds is sheared to align the seeds in the casting direction.

In the FDC process, the material to deposit is sheared both during filament fabrication and deposition of material through fine nozzles. We have explored the possibility of TGG in bismuth titanate (BiT) system using the manufacturing process of FDC. BiT filament with fine BiT powder and 5 wt.% platelet seeds were developed. On the surface of the filaments, seeds were all aligned in the extrusion direction, whereas in the bulk of the filament, the platelet seeds were almost randomly oriented.[17]

Improved orientation of the seeds was obtained in the deposited samples due to the fine slice thickness of 250 μm. With such thin layers, the shear stresses were higher and more uniform, resulting in better alignment of the seeds. Green FDC samples were heated to remove the organic and then to sinter and induce grain growth and orientation. The X-ray diffraction and microstructure of the sintered samples showed that partial orientation was obtained, with the calculated Lotgering factor[18] of 0.46 (Fig. 4). Currently, further work is in progress to improve the orientation of the sintered BiT parts.

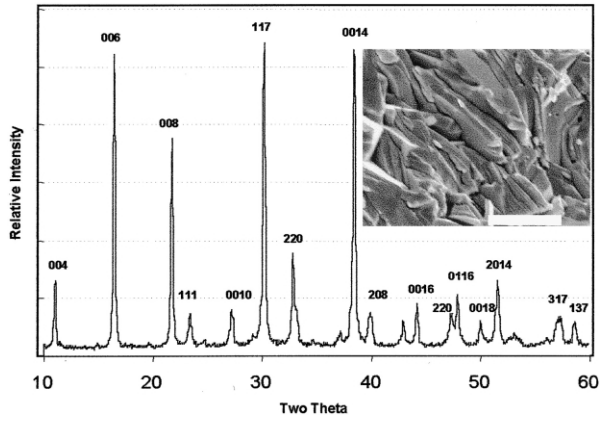

Fig. 4. X-ray diffraction from the surface of an FDC-BiT sample, illustrating the high intensity of (00L) planes resulting from grain orientation. Fracture surface of the sample also shows partial grain orientation (5 μm bar).

5. Photonic bandgap structures

Photonic bandgap (PBG) structures are periodic dielectric structures with alternate high and low permittivity materials in order to have an electromagnetic stop-band in a desired direction.[19] A variety of potential applications such as thresholdless lasers, high quality single mode LEDs, and microwave antennas are already being explored.

We have implemented fused deposition of multi-materials to make a variety of PBG parts with different dimensions according to the results obtained from simulation work.[20] Fig. 5 shows an alumina PBG structure with square-section rods. A wide gap existed between the alumina rods, therefore, a support material was needed to avoid sagging during deposition. An FDC wax (ICW05) was deposited in the gaps to be able to finish deposition without any distortion in the part. The wax was later removed at low temperature of 110°C, and the part was heated to remove the organics and finally to sinter the structure at 1600°C. Simulation works suggest that such a PBG structure provide a band gap in the frequency range of 8–12 GHz.[20]

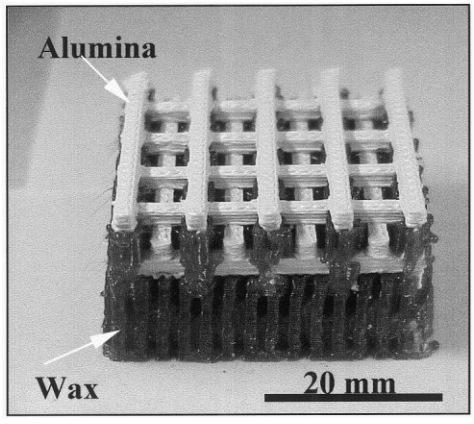

Fig. 5. A photonic bandgap structure made with alumina and wax (as a support material during deposition). After organic removal and sintering, a periodic structure of square alumina rods is obtained.

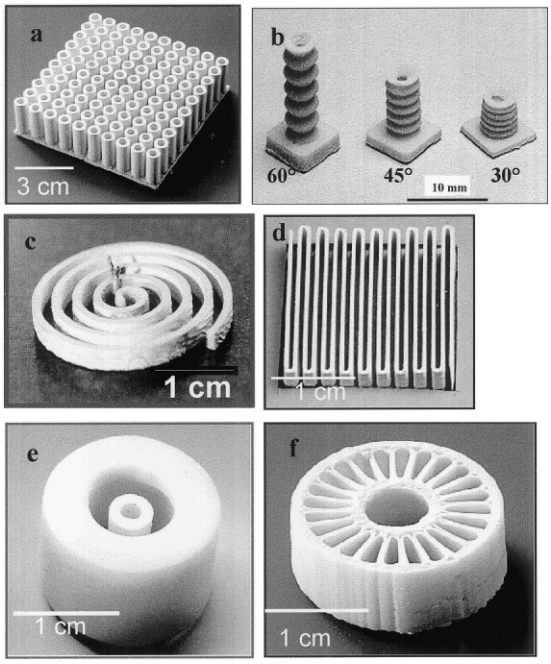

Fig. 6. Variety of transducers made by FDC: (a) 10×10 tube array; (b) bellows; (c) spiral; (d) curved transducer; (e) telescoping; (f) radial actuators.

6. Transducers fabricated by FDC

Piezoelectric ceramics and ceramic/polymer composites with novel designs have been fabricated for sensor and actuator applications.[21,22] The FDC process allows rapid manufacturing of new designs. In addition, the electromechanical properties of such components can be easily tailored by changing the shape and spatial distribution of the ceramic material. Fig. 6 shows photographs of several transducer designs, two of which (tube and spiral actuators) are briefly presented below.

Tube actuators. Tube and tube array PZT structures were fabricated for actuator, broadband resonant transducer, and sensor applications. Single tube and tube arrays were fabricated with the dimensions of 3 to 8 mm outer diameters, 6 to 20 mm heights, and 0.4 to 2.0 mm wall thicknesses. Moreover, tube actuators with zigzag wall design (bellows) with three angles of 30, 45, and 60 have been designed and fabricated. The deposition process showed that the high angle bellows of 45 and 60° could be successfully deposited while the 30° bellows could not be made without flaws due to the lack of support and weak bonding between neighboring layers. In comparison with the straight tubes, bellows showed up to 50% larger radial displacements, whereas the displacement along the height was about 20–30% lower in bellows than that of the straight tubes.

Tube actuators with helical electrodes were fabricated to determine the possibility of enhancing displacement along the tube height. Such tubes were made of a piezoelectric material (e.g. PZT, PMN–PT, etc.) and silver–palladium electrode. Two different designs were considered. In the first design, the helical electrodes were located within the tube wall. Such tubes were fabricated using a fused deposition of multi-material (FDMM) machine in a single deposition step. In order to make the second design, a two-step deposition was used; initially simple tubes were deposited, and then the helical electrodes were placed on the surface in the next step. The oxidation/reduction of silver–palladium electrode during binder removal and sintering in air caused extensive expansion/shrinkage and therefore, damages to the tubes. Fig. 7 shows the TGA curve of the electrode filament, illustrating binder loss in the tempera-

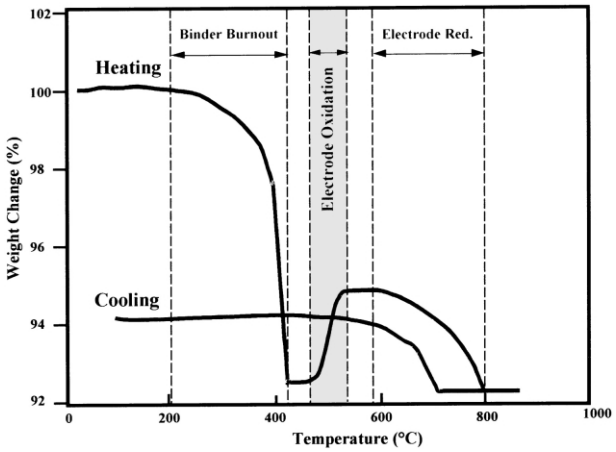

Fig. 7. Thermogravimetry analysis of silver–palladium filament in air at heating rate of 600°C/h, showing binder removal, and subsequent weight gain and loss due to oxidation and reduction of palladium. The porous electrode oxidizes partially upon cooling.

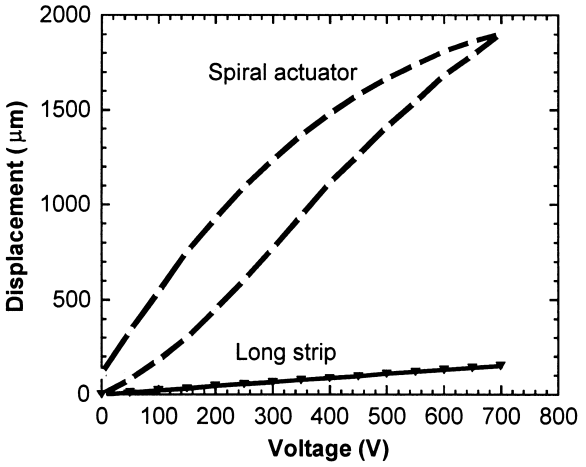

Fig. 9. Tangential displacement of a spiral actuator as a function of driving voltage in comparison with the d_{31} response of a straight PZT strip of the same dimensions.

ture range of 200–430°C, followed by weight gain (460–530°C) and weight loss (580–800°C) resulted from the oxidation and reduction of palladium. The increase and decrease of the electrode (palladium) weight corresponds to volume gain (oxidation) of palladium and volume loss (reduction) of palladium oxide, respectively. A new electrode filament with pre-oxidized silver–palladium powder is currently under development. The preliminary results showed much less damages compared to the regular electrode material (Fig. 8). The post-FDC processing steps are now being modified to obtain defect-free sintered tubes.

Spiral actuators. A new actuator with spiral geometry (high length-to-width ratio) was developed in order to obtain high displacement utilizing the d_{31} coefficient.[23] When an electric field was applied to a spiral actuator in the poling direction (across the width), the spiral tip displaced in both tangential and radial directions. The tangential displacement was in millimeter range, whereas the radial movement was relatively small in the order of a few microns. Fig. 9 shows a typical tangential displacement of a spiral actuator as a function of dc driving voltage in comparison with the transverse displacement of a long strip of the same length, width, and height as the spiral.

The spiral consisted of 5 turns with an external diameter of 32 mm. The effective length, width, and height of the spiral were 280, 0.6, and 2.75 mm, respectively. The spiral and the PZT strip were driven under dc bias, in the same direction as they were poled, up to 700 V (~11.6 kV/cm) with 50 V increments. A maximum lateral displacement of 153 μm was measured in the long strip caused by transverse (d_{31}) piezoelectric coefficient actuation.

The PZT spiral actuator exhibited a displacement of 1900 μm, which is more than 12 times larger than that of the long strip under the same voltage. This suggests that the d_{31} effect (transverse strain) be of minor importance for the observed displacement in spiral actuators. The actuator exhibited a much larger displacement when driven in ac mode at resonance frequency, reaching about 7500 μm at 100 Vac. Such amplification is very important for applications in piezoelectric motors, where the actuators operate in resonance mode.

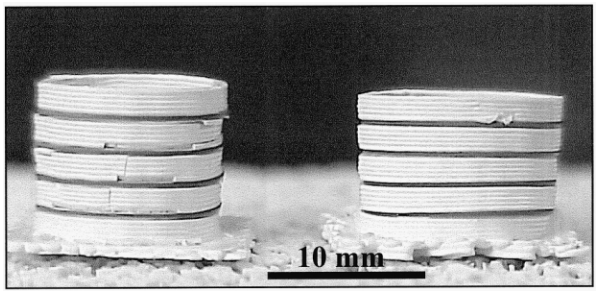

Fig. 8. Multilayer tube actuators upon the completion of binder removal at 550°C in air. The tubes are made of PMN–PT and electrode materials. The tube made with ordinary electrode filament (left) shows severe cracking and delamination whereas the tube made with the pre-oxidized electrode (right) does not show any cracking.

7. Summary

Fused deposition of ceramics (FDC) has been used to prototype a variety of ceramic components. The ECG9 binder exhibits properties suitable for fused deposition and for incorporation of a variety of ceramic and metal powders. A number of filaments such as PZT, PMN, alumina, and BiT have been made, and successfully used in the FDC process. A high temperature silver–palladium electrode filament has been developed for the fabrication of electromechanical components. The performance of filaments in the FDC process was characterized through a process map using the compressive moduli and viscosities of the materials at deposition

temperatures. Photonic bandgap structures with alumina rods were fabricated with alumina and wax as a support material for microwave and laser applications. Net shape BiT components with a small volume of platelet seeds were deposited and TGG-annealed to induce grain orientation. Many novel actuators, including spiral with giant displacement, were developed via FDC route.

Acknowledgements

The authors would like to thank F. Mohammadi, N. Venkataraman, and T.F. McNulty for their hard work and contribution to this article. This work is financially supported by ONR under grant Nos. N00014-96-1-0959, N00014-96-1-1175, and N00014-99-1-0470.

References

1. Hull, C. W., Method for production of 3-D objects by stereolithography. US Patent No. 4,929,402, issued May 29, 1990.
2. Beaman, J. and Deckard, C. R., Selected Laser Sintering with Assisted Power Handling. US Patent No. 4,938,816, issued June 3, 1990.
3. Comb, J. W. and Priedeman, W. R., Control parameters and materials selection criteria for rapid prototyping systems. In *Proceedings of the Solid Freeform Fabrication Symposium*, ed. H. L. Marcus, J. J. Beaman, J. W. Barlow, D. L. Bourell and R. H. Crawford. The University of Texas at Austin, Austin, Texas, 1993, pp. 86–91.
4. Sachs, E. M., Cima, M. J., Williams, P., Brancazio, D. and Cornie, J., Three dimensional printing: rapid tooling and prototypes directly from a CAD model. *J. Eng. Ind.*, 1992, **114**, 481–488.
5. Micropen Technology, Ohmcraft, Inc., Brochure.
6. Griffith, M. L. and Halloran, J. W., Freeform fabrication of ceramics via stereolithography. *J. Am. Ceram. Soc.*, 1996, **79**, 2601–2608.
7. Agarwala, M. K., Bandyopadhyay, A., van Weeren, R., Whalen, P., Safari, A. and Danforth, S. C., Fused deposition of ceramics: rapid fabrication of structural ceramic components. *Am. Ceram. Soc. Bull.*, 1996, **75**, 60–65.
8. Bandyopadhyay, A., Panda, R. K., Agarwala, V. F., Danforth, S. C. and Safari, A., Processing of piezocomposites by fused deposition technique. *J. Am. Ceram. Soc.*, 1997, **80**, 366–1372.
9. Danforth, S. C. Agarwala, M., Bandyopadghyay, A., Langrana, N., Jamalabad, V. R., Safari, A. and Weeren, R., Solid Freeform Fabrication Methods. United States patents, 1998, 5, 738,817.
10. Jafari, M. A., Han, W., Mohammadi, F., Safari, A., Danforth, S. C. and Langrana, N., A novel system for fused deposition of advanced multiple ceramics. *Rapid Prototyping Journal*, 2000, **6**(3), 161–175.
11. McNulty, T. F., *Prototyping of radially oriented piezoelectric ceramic-polymer tube composites using fused deposition and lost mold processing techniques*. PhD thesis, Department of Ceramic and Materials Engineering, Rutgers University, 1999.
12. McNulty, T. F., Mohammadi, F., Bandyopadghyay, A., Shanefield, D. F., Danforth, S. C. and Safari, A., Development of a binder formulation for fused deposition of ceramics. *Rapid Prototyping Journal*, 1998, **4**(4), 144–150.
13. McNulty, T. F., Shanefield, D. F., Danforth, S. C. and Safari, A., Dispersion of lead zirconate titanate for fused deposition of ceramics. *J. Am. Ceram. Soc.*, 1999, **82**(7), 1560–1575.
14. Safari, A., Danforth, S. C., Jafari, M. A., Allahverdi, M., Jadidian, B., Mohammadi, F., Vankataraman, N. and Rangarajan, S. Fabrication of advanced functional ceramics by fused deposition technique. *Proceedings of the 9th European Conference on Rapid Prototyping and Manufacturing*, 17–19 July, 2000, Athens, Greece, pp. 247–263.
15. Seabaugh, M. M., Kerscht, I. H. and Messing, G. L., Texture development templated grain growth in liquid-phase-sintered α-alumina. *J. Am. Ceram. Soc.*, 1997, **80**(5), 1181–1188.
16. Horn, J. A., Zhang, S. C., Selvaraj, U., Messing, G. L., Trolier-McKinstry, S. and Yokoyama, M., Fabrication of textured $Bi_4Ti_3O_{12}$ by templated grain growth. *J. Am. Ceram. Soc.*, 1999, **82**(4), 921–926.
17. Allahverdi, M., Jadidian, B., Ito, Y. and Safari, A., Fabrication of bismuth titanate components with oriented microstructures via FDC and TGG. In *Proceedings of the 12thIEEE International Symposium on the Applications of Ferroelectrics*. Hawaii, 29 July–2 August, 2000.
18. Lotgering, F. K., Topotactical reactions with ferrimagnetic oxides having hexagonal crystal structures — I. *J. Appl. Phys.*, 1968, **39**(5), 2268–2274.
19. Yablonovitch, E., Photonic band-gap structures. *J. Opt Soc. Am.*, 1993, **10**(2), 283–295.
20. Chen, Y., Bartzos, D., Liang, S., Lu, Y., Safari, A., Danforth, S. C., Allahverdi, M. and Pilleux, M. E., Three-dimensional alumina photonic bandgap structures: numerical simulation and fabrication by fused deposition of multimaterials. In *Proceedings of the Solid Freeform Fabrication Symposium*. The University of Texas at Austin, Austin, Texas, August 2000.
21. Janas, V. F. and Safari, A., Overview of fine scale piezoelectric ceramic/polymer composite processing. *J. Am. Ceram. Soc.*, 1995, **78**(11), 2945.
22. Safari, A., Development of piezoelectric composites for transducers. *J. Phys III France*, 1994, **4**, 1129.
23. Mohammadi, F., Kholkine, A. L., Jadidian, B. and Safari, A., High-displacement spiral piezoelectric actuators. *Applied Physics Letters*, 1999, **75**(16), 2488–2490.